# Synthesis of low shrinkage monolith alumina aerogels by surface modification and ambient pressure drying

*Chi Li[1], Zheng Gong[2], Likang Ding[1], Donglai Guo[3], Wenbin Hu[3] ✉*

[1]*School of Materials Science and Engineering, Wuhan University of Technology, Wuhan 430070, People's Republic of China*
[2]*FiberHome Technologies Group, Wuhan 430205, Hubei, People's Republic of China*
[3]*Key Laboratory of Fiber Optic Sensing Technology and Information Processing, Ministry of Education, Wuhan University of Technology, Wuhan 430070, People's Republic of China*
✉ *E-mail: wenbinhu_whut@163.com*

Published in Micro & Nano Letters; Received on 8th March 2018; Revised on 25th April 2018; Accepted on 16th May 2018

The authors have synthesised a kind of low shrinkage alumina ($Al_2O_3$) aerogel using an inexpensive salt of aluminium ($AlCl_3{\cdot}6H_2O$) via tetraethoxysilane modification and an ambient pressure drying process. The morphology, pore structure, surface group, crystal phase and thermal properties of the $Al_2O_3$ aerogel are analysed by X-ray diffractometer, scanning electron microscopy, Fourier transform infrared spectra and nitrogen adsorption test. Further improvement in thermal stability and thermal shrinkage are obtained by incorporation of silicon (Si) atoms during the aerogel preparation. The specific surface area of modified aerogel is 480 $m^2/g$ and the diameter shrinkage is 8% after drying, and reach 304 $m^2/g$ and 16.5% after heating at 1000°C. The approach, which is straightforward, inexpensive and safe, can be employed to prepare a monolithic mesoporous material with low shrinkage and high-temperature resistance. This will further promote the potential application of packaging and thermal insulation materials.

**1. Introduction:** Aerogels are highly porous materials with a series of unique physical properties [1–4]. Owing to these properties, aerogels can be promising candidates for thermal insulations, heat-storage systems, acoustic devices, luminescent solar systems, catalysts and catalyst support etc. [5–8] Since 1930s, Kistler [9] first produced silica aerogels, many types of aerogels have been successfully synthesised such as carbon, Si dioxide ($SiO_2$), titanium dioxide ($TiO_2$) and $Al_2O_3$ [10–13]. Among all of the types of aerogels, alumina aerogels have attracted increasing attention because of their relatively high strength, enhanced thermal stability and chemical durability [14–16]. In particular, the volume shrinkage after heat treatment is one of the key issues for package materials to insulate extra strain caused by shrinkage on the packaged objectives. The synthesis of the alumina aerogel involves three major steps: (i) preparation of wet gel with nanoporous structure; (ii) ageing the gel to enhance the skeleton structure; and (iii) drying the wet gels to remove the trapped solvent from the pores of the gels. Supercritical drying, as a conventional method to prepare monolithic aerogel, requires high-pressure equipment with high risk and cost [17–20]. It severely restricts the industrial production of aerogel. In recent years, ambient pressure drying (APD) has been used to produce aerogels with less risk and cost. Baumann reported the monolithic alumina aerogels with low density (60–130 $kg/m^3$) and high surface area (600–700 $m^2/g$) [21]. Poco synthesised high porosity (98% porous) monolithic alumina aerogel and found that the compression modulus is only 0.55 MPa [13]. Wu has reported the hydrophobic alumina aerogel monolithic, using trimethylmethoxysilane (TMMOS)/hexanes solution as a modifier and APD [22].

In this Letter, we synthesised the monolith alumina aerogels with low shrinkage by APD method, by employing the cheap inorganic salt ($AlCl_3{\cdot}6H_2O$) as a precursor, tetraethoxysilane (TEOS) as a modifier. The relatively low volume shrinkage and high thermal stability of monolith alumina aerogels were obtained. The surface modification was carried out by using TEOS to introduce the Si atoms on the surface of the alumina, which successfully suppressed $\alpha$-alumina phase transformation [23]. Thereby, the aerogels shrinkage after heat treatment was suppressed and the moldability after heat treatment was highly improved.

**2. Experimental results**

2.1. Preparation: To synthesise the aerogels, aluminium chloride hexahydrate ($AlCl_3{\cdot}6H_2O$) was used as the alumina source, TEOS as a modifier, ethanol as a solvent, propylene oxide (PO) as a network forming agent, formamide (FA) as a chemical drying control agent and N-hexane as exchange solvent from the wet gels. All chemical reagents were analytical grade and supplied by Sinopharm Group Chemical Reagent Co., Ltd.

$AlCl_3{\cdot}6H_2O$, deionised water, ethanol and FA (molar ratios $AlCl_3{\cdot}6H_2O$:$H_2O$:ethanol:FA = 1:14:10:0.8) were stirred at 50°C for 70 min and then cooled to room temperature. After hydrolysis for 40 min, PO (molar ratios $AlCl_3{\cdot}6H_2O$:PO = 1:8) was poured into the clear solution. After waiting for 2–5 min, the alcohol solution which has not been gelatinised was rapidly poured into an injection vessel with a diameter of 30 mm. The alumina wet gels were sealed in the vessel for drying process for the following gelation.

After the container was covered by a plastic cover and the gel was aged at room temperature for 12 h, the wet gel samples were immersed in a bath of ethanol at 40°C for 12 h to exchange the water and reaction by-products from the pores of the materials. The surface modification was carried out by immersing the gels in 40 and 80% V TEOS/ethanol solution at 40°C for 12 h. Then, the gels were soaked in ethanol and hexane at 40°C for 12 h in order to remove the unreacted TEOS. After drying at room temperature for 24 h under ambient pressure, the gels were dried in a dry box at 40°C (2 h) – 60°C (2 h) – 80°C (2 h) – 105°C (2 h) to obtain white monolith alumina aerogels. Three samples were investigated mainly in this Letter. Sample A1 was used as a blank sample without TEOS modification. Sample A2 was obtained after modification of 40% V TEOS/ethanol solution. Moreover, sample A3 was the one with modification of 80% V TEOS/ethanol solution. The 40% V TEOS/ethanol solution and 80% V TEOS/ethanol solution are denoted as 40 and 80% T/E, respectively.

2.2. Characterisations: Scanning electron microscopy (SEM) was conducted using a JEM2100F field emission scanning electron microscope by operating at 3 kV to measure the microstructure of the samples. Fourier transform infrared spectra (FTIR) were carried


© The Institution of Engineering and Technology 2018

doi: 10.1049/mnl.2018.5077

out by using a NicoletNexus 670 FTIR spectrometer to analyse the organic groups in aerogel. Surface area and pore volume were measured by using a Micromeritics ASAP2020 surface area and pore distribution analyser after the samples were degassed in vacuum at 90°C for 6 h. The specific surface area was calculated using the Brunauer-Emmett-Teller (BET) equation. The pore size distribution was calculated from the data of the adsorption branch of the isotherm using Barrett–Joyner–Halenda method. The crystal phase of the sample was measured with an X-ray diffractometer (XRD, D8 Advance, Germany) with a rated output power of 3 kW, a $2\theta$ rotation range of $-10°$ to 168°, a goniometer radius of ≥200 mm, and an angle reproducibility of 0.001°. The apparent density of the sample was calculated using the formula $\rho = m/V$ ($\rho$ is the aerogel density, $m$ is its mass and $V$ is its volume).

## 3. Results and discussion

3.1. Morphology analysis of sample in heat-treatment process: The volume shrinkages are investigated by measuring the diameter variations of the samples A1, A2 and A3 obtained at ambient pressure after heat treatment at different temperatures. The trend of the diameter shrinkage is calculated by the equation $\Delta D/D_0$. Fig. 1 shows that macroscopic morphology and diameter variation of sample A1 (unmodified alumina aerogels), sample A2 (modified by 40% T/E) and sample A3 (modified by 80% T/E) before and after heat treatments at 600°C and subsequently at 1000°C, respectively. As shown in Fig. 1*a*, the diameter of sample A1 (unmodified alumina aerogels) varies from 21.84 (no heating) to 17.63 mm (600°C) and 14.81 mm (1000°C), with diameter shrinkage ratios of 19.3 and 32.2%, respectively, compared with the initial diameter. Fig. 1*b* shows that the diameter of sample A2 varies from 22.05 to 18.59 and 17.58 mm, with shrinkage ratios of 15.7 and 20.3%, respectively. Fig. 1*c* shows that the diameter of sample A3 varies from 27.4 to 24.08 and 22.8 mm, with shrinkage ratios of 12.1 and 16.5%, respectively. It can be found that the diameter shrinkage after heat treatments at 600 and 1000°C of TEOS modified samples A2 and A3 is smaller than that of unmodified sample A1. It is noted that the shrinkage ratio was significantly reduced for sample A3, compared with the unmodified sample A1. This is due to the introduction of Si, which can effectively improve the structural strength and heat resistance of aerogels. To clarify the trend of shrinkage, the diameter variation is summarised in Fig. 2*a* and the diameter shrinkage ratio in Fig. 2*b*.

To clarify the influence of TEOS modification, following characterisation methods are complemented on samples A1 and A3.

3.2. Analysis of surface microscopic morphology: The microstructure and particle morphology of samples A1 (unmodified) and A3 (80% T/E modified) were examined by using SEM. Fig. 3 depicts the SEM images of samples A1 and A3 after calcined at 900°C for 2 h. Before heat treatment, the unmodified alumina aerogels, sample A1, exhibit a loose and porous structure with less connectivity. The network structure is formed by homogeneous spherical particles with small pores, which have diameters of ~150 nm (as shown in Fig. 3*a*). After heating at 900°C for 2 h, and the aerogel particles became more compact, and the agglomeration occurred between the particles. The porosity was decreased and a small amount of large pore with diameters >500 nm emerge in the aerogel (as shown in Fig. 3*b*). This is due to the fact that

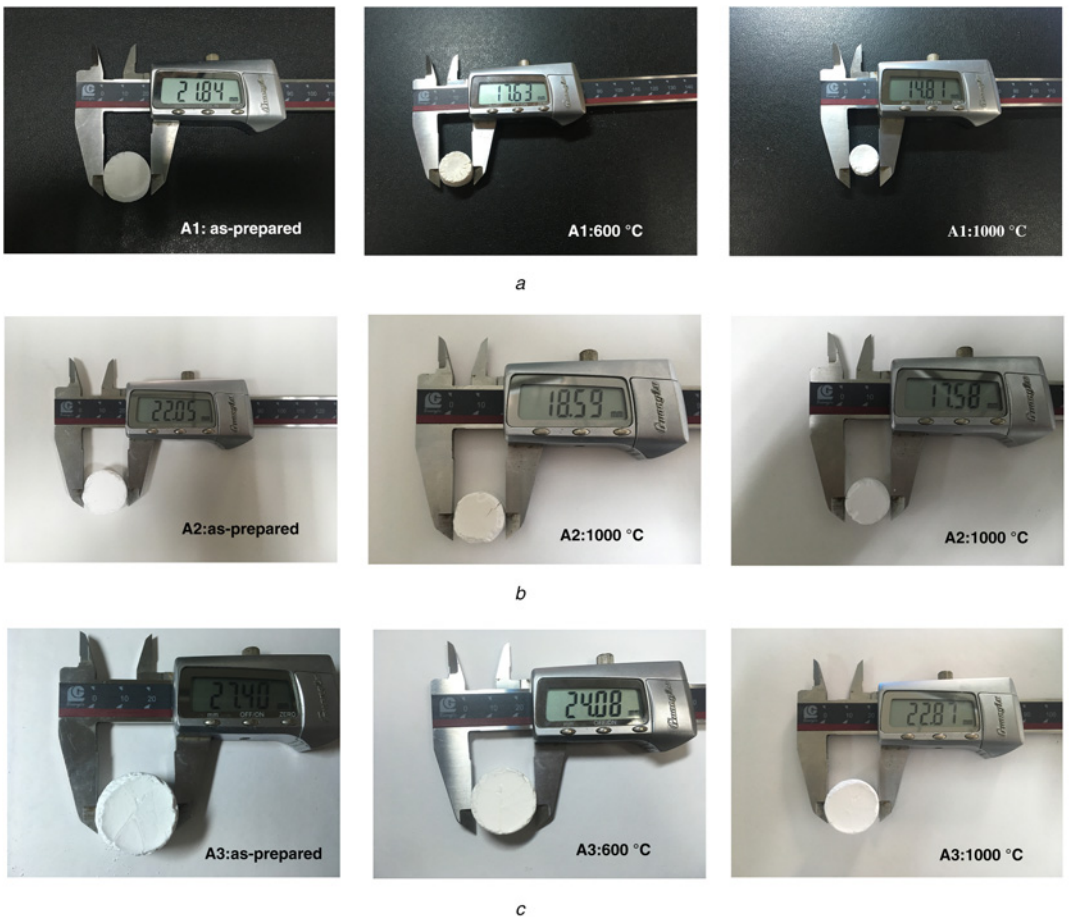


**Fig. 1** *Photograph of aerogel before and after heat treatments*
*a* Sample A1
*b* Sample A2
*c* Sample A3



© The Institution of Engineering and Technology 2018

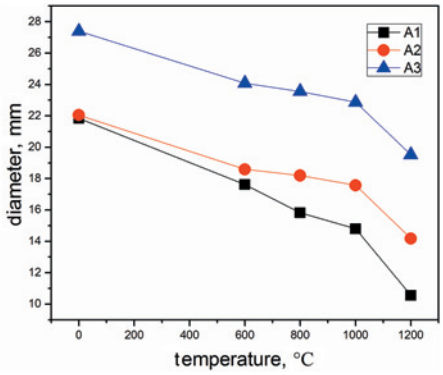


**Fig. 2** *Diameter change and shrinkage change of the aerogels*
*a* Before heat treatment at different temperatures
*b* After heat treatment at different temperatures

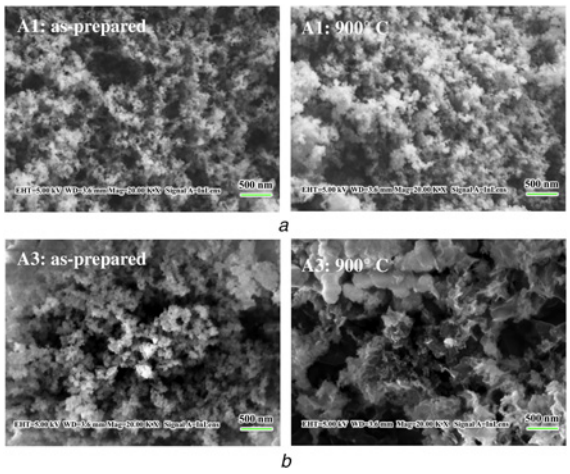


**Fig. 3** *SEM images of the aerogels before and after heat treatments at 900°C*
*a* Sample A1 (without modification)
*b* Sample A3 (80% T/E modified)

after heating, the nanoporous structure collapses and the microstructure becomes denser, resulting in a shrunken volume. Compared to the unmodified aerogels, the pore size of microstructure for sample A3 was larger, with diameters of 200–400 nm. After heating at 900°C for 2 h, some of the pores are clogged, another forms large pores. However, serious collapse did not occur, and the porous skeleton was maintained. As a result, the diameter shrinkage of sample A3 is relatively small after high-temperature treatment.

3.3. Fourier TIR spectroscopy: The influence of TEOS on the surface functional groups of samples A1 and A3 was verified by FTIR, as shown in Fig. 4. The most distinct peaks are located at 3439 and 1641 $cm^{-1}$, which are commonly related to the stretching vibrations of O–H bond and H–O–H bond. These two bonds do not change significantly before and after surface modifications, indicating that both aerogel samples contain hydroxyl and physical water adsorption. It can be seen from Fig. 4 that the absorption peaks at 1060, 619 and 450 $cm^{-1}$, which represent the boehmite structure, exist in both spectra. The presence of boehmite in both samples can be revealed. With TEOS modification, the intensity of the absorption peak related to boehmite phase is enhanced. At the position of 1060 $cm^{-1}$, the absorption peak intensity increases obviously, indicating the Al–O–Al stretching vibration is more obvious. This is due to the formation of Al–O–Si bond.

3.4. XRD analysis: The evolution of different phases by varying heating temperature was found from the XRD analysis. Fig. 5*a*

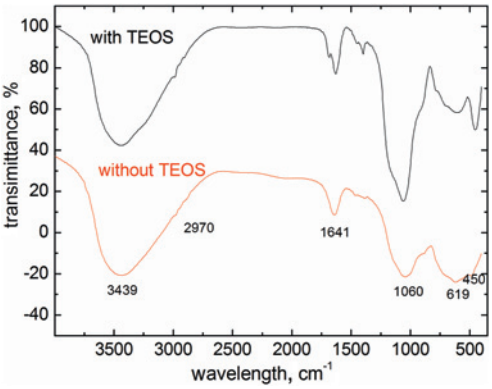


**Fig. 4** *FTIR spectra of aerogel sample A1 (without modification) and A3 (80% T/E modified)*

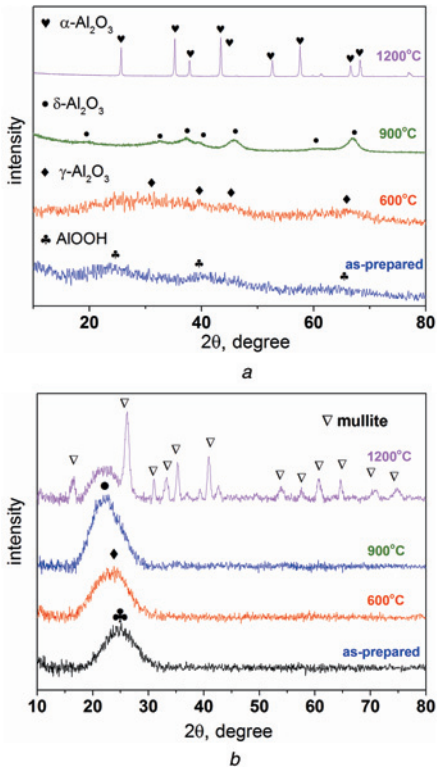


**Fig. 5** *XRD patterns of the aerogels before and after heat treatments*
*a* Sample A1
*b* Sample A3


© The Institution of Engineering and Technology 2018

doi: 10.1049/mnl.2018.5077

provides the XRD patterns of unmodified alumina aerogels (sample A1), which is heat treated at different temperatures (as prepared, 600, 900 and 1200°C). The as-prepared sample shows diffraction weak peaks at 27°, 39° and 65°, which corresponds to boehmite. After heat treatment at 600°C for 2 h, the $\gamma$-$Al_2O_3$ pattern begins to emerge. When the temperature was increased to 900°C, the pattern shows clear diffraction peaks at 19°, 32°, 37°, 39°, 46°, 60° and 67°, representing a significant $\delta$-$Al_2O_3$ phase morphology in the alumina aerogel. When the temperature reaches 1200°C, the alumina aerogels exhibit a very significant $\alpha$-$Al_2O_3$ crystalline structure. Compared to other $Al_2O_3$ crystal forms (spinel structure), the transition to $\alpha$-$Al_2O_3$ phase (hexagonal close packed structure) causes volume shrinkage and sintering, which decreases the thermal insulation performance of alumina aerogel. Fig. 5*b* provides the XRD patterns of sample A3. It can be seen from the figure that the XRD curve of the aerogel is a diffused diffraction peak, showing an amorphous boehmite structure. After heat treatment at 600 and 900°C, the aerogel is still amorphous and pseudo-boehmite. The addition of Si, as a result of TEOS modification, is effective in inhibiting the phase transition of aerogel. Therefore, the thermal stability of aerogel is improved and the volume shrinkage caused by phase transition is suppressed. After heat treatment at 1200°C for 2 h, the aerogel shows mullite phase ($3Al_2O_3{\cdot}2SiO_2$) which prevents the formation of $\alpha$-$Al_2O_3$ crystal structure and improved the thermal stability of aerogels.

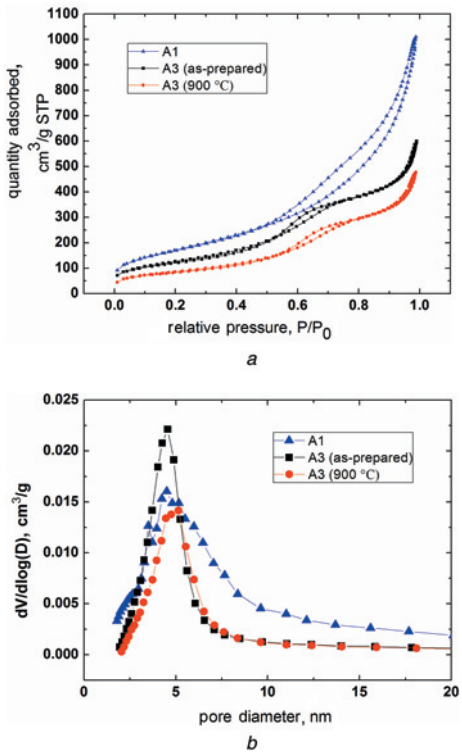


**Fig. 6** *Nitrogen adsorption*
*a* $N_2$ adsorption–desorption curve
*b* Pore size distribution of the aerogel samples

3.5. Nitrogen adsorption: The nitrogen adsorption–desorption isotherms and pore size distributions of three specimens are measured. One is from sample A1 (as prepared) and two are from sample A3 (as prepared and heat treatment at 900°C), as shown in Fig. 6. It can be seen from Fig. 6*a* that there are hysteresis loops in the adsorption and desorption curves of the three specimens, and the nitrogen physisorption isotherms obtained for all specimens exhibited Type IV hysteresis loops. Comparing the curves of sample A3 without heating and with heat treatment, the lagging ring is only slightly narrowed and the change is not obvious, which shows that the doping of Si makes the aerogel thermal stability enhanced. When the pressure is relatively divided into the high-pressure zone, it can be found that the curve of sample A3 has a slow platform, which shows that the pore size distribution of the aerogel with TEOS modification is more uniform.

Fig. 6*b* shows the pore size distributions of sample A1 and sample A3 (as prepared and heat treatment at 900°C). It can be found that the main pore diameters of the three specimens are below 50 nm and the main pore size is centred approximately at 5 nm. The pore size distribution of aerogel sample with TEOS modification is narrower and the pore size distribution is more uniform around 5 nm. The negative effects of aerogel in the capillary pressure difference can be reduced to a certain extent. The parameters of pore structures for three specimens are summarised in Table 1. The specific surface areas of samples A1 and A3 without heating and A3 with heating at 900°C are 631, 480 and 308 $m^2/g$, respectively. The porosity of alumina aerogels with TEOS modification is reduced due to the infiltration of Si, by blocking the gap and the introduction of nitrogen, resulting in less nitrogen adsorption. After heat treated at 900°C for 2 h, the surface area of sample A3 is 308 $m^2/g$, the specific surface area of the alumina aerogels prepared in [23] after heating at 1000°C was near 100 $m^2/g$. The specific surface area of the alumina aerogels in [24] after heat treatment at 1200°C was 147 $m^2/g$. Compared to the above literature, the alumina aerogels in this Letter after TEOS modification and heated at 900°C can still maintain a relatively high specific surface area, indicating that the incorporation of Si increases the high-temperature resistance and thermal stability of the aerogel.

3.6. Mechanism of surface modification: The surface modification of alumina gel by TEOS/ethanol solution is manifested in the hydroxyl reaction of TEOS and gel skeleton, gel skeleton grafted with Si bond. The modification mechanism is shown in Fig. 7. It can be seen that TEOS and gel surface produce –Al–O–Si– bond. The modification of TEOS, by interlinking into a chain structure, plays a supporting role on the connection of the gel pores, thereby reduces the shrinkage during the drying process caused by the capillary. At the same time, the incorporation of Si can effectively resist the change of the gas phase transition of the aerogels during the heat treatment. Moreover, it can further improve the temperature resistance of

**Table 1** Texture properties of the alumina aerogels

| Specimens | Compositions | Density, $kg/m^3$ | Specific area, $m^2/g$ | Main pore size, nm | Pore volume, $cm^3/g$ |
|---|---|---|---|---|---|
| A1 | without modification | 113 | 631 | 4.50 | 1.1516 |
| A3 (as prepared) | 80% T/E modified | 133 | 480 | 4.56 | 0.7379 |
| A3 (900°C) | 80% T/E modified | 203 | 308 | 5.15 | 0.9270 |



© The Institution of Engineering and Technology 2018

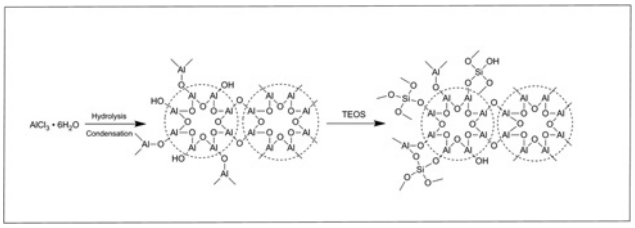


**Fig. 7** *Schematic illustration for TEOS modification mechanism*

the alumina aerogels, which results in the shrinkage reduction during the heat treatment.

**4. Conclusions:** Monolithic alumina aerogel with low shrinkage is synthesised via TEOS modification and an ambient pressure dry process. The modification contributes to the production of –Al–O–Si– bond by the incorporation of Si, which enhanced the gel framework and suppresses the phase transition of $Al_2O_3$ at elevated temperature. Compared to the unmodified sample, the diameter shrinkage of 80% V TEOS/alcohol solution modified simply reduced by 50% at 1000°C (16.5%), and a loose and porous microstructure is maintained. As a result of the suppression of the phase transition, the modified sample maintains large specific surface area (308 $m^2$/g) after heating at 1000°C. The results contribute to the large-scale industrial production of low shrinkage alumina aerogel. Moreover, the relatively low shrinkage of the aerogel during heat treatment will be beneficial potentially for strain insulation from the package material to the protected objectives.

**5. Acknowledgments:** This work was supported by National Science Foundation of China (NSF) (grant nos. 51672199, 61402345), and the Nation Key Research and Development Program of China (grant no. 2017YFB0405501).

## 6 References

[1] Gurav J.L., Jung I.-K., Park H.-H., *ET AL.*: 'Silica aerogel: synthesis and applications', *J. Nanomater.*, 2010, **2010**, pp. 1–11
[2] Yang X., Wei J., Shi D., *ET AL.*: 'Comparative investigation of creep behavior of ceramic fiber-reinforced alumina and silica aerogel', *Mater. Sci. Eng. A*, 2014, **609**, pp. 125–130
[3] Hrubesh L.W.: 'Aerogel applications', *J. Non-Cryst. Solids*, 1998, **225**, pp. 335–342
[4] Pierre A.C., Pajonk G.M.: 'Chemistry of aerogels and their applications', *ChemInform*, 2002, **102**, p. 4243
[5] Al-Yassir N., Le Van Mao R.: 'Thermal stability of alumina aerogel doped with yttrium oxide, used as a catalyst support for the thermocatalytic cracking (TCC) process: an investigation of its textural and structural properties', *Appl. Catal. A, Gen.*, 2007, **317**, pp. 275–283
[6] Smith D.M., Maskara A., Boes U.: 'Aerogel-based thermal insulation', *J. Non-Cryst. Solids*, 1998, **225**, pp. 254–259
[7] Xiao L., Grogan M.D.W., England R., *ET AL.*: 'Stable low-loss optical nanofibres embedded in hydrophobic aerogel', *Opt. Express*, 2011, **19**, p. 764
[8] Hilonga A., Kim J.-K., Sarawade P.B., *ET AL.*: 'Low-density TEOS-based silica aerogels prepared at ambient pressure using isopropanol as the preparative solvent', *J. Alloys Compd.*., 2009, **487**, pp. 744–750
[9] Kistler S.S.: 'Coherent expanded aerogels and jellies', *Nature*, 1931, **127**, p. 741
[10] Wang Y., Zou Y., Chen J., *ET AL.*: 'A flexible and monolithic nanocomposite aerogel of carbon nanofibers and crystalline titania: fabrication and applications', *RSC Adv.*, 2013, **3**, pp. 24163–24168
[11] Leventis N., Sotiriouleventis C., Guohui Zhang A., *ET AL.*: 'Nanoengineering strong silica aerogels', *Nano Lett.*, 2002, **2**, pp. 957–960
[12] Balakumar K., Kalaiselvi N.: 'High sulfur loaded carbon aerogel cathode for lithium– sulfur batteries', *RSC Adv.*, 2015, **5**, pp. 34008–34018
[13] Poco J.F., Satcher J.H.Jr., Hrubesh L.W.: 'Synthesis of high porosity, monolithic alumina aerogels', *J. Non-Cryst. Solids*, 2001, **285**, pp. 57–63
[14] Zu G., Shen J., Wei X., *ET AL.*: 'Preparation and characterization of monolithic alumina aerogels', *J. Non-Cryst. Solids*, 2011, **357**, pp. 2903–2906
[15] Wu X., Shao G., Cui S., *ET AL.*: 'Synthesis of a novel $Al_2O_3$–$SiO_2$ composite aerogel with high specific surface area at elevated temperatures using inexpensive inorganic salt of aluminum', *Ceram. Int.*, 2016, **42**, pp. 874–882
[16] Ji L., Lin J., Tan K.L., *ET AL.*: 'Synthesis of high-surface-area alumina using aluminum tri-sec-butoxide-2,4-pentanedione-2-propanol-nitric acid precursors', *Chem. Mater.*, 2000, **12**, pp. 931–939
[17] Grader G.S., Rifkin Y., Cohen Y., *ET AL.*: 'Preparation of alumina aerogel films by low temperature $CO_2$ supercritical drying process', *J. Sol-Gel Sci. Technol.*, 1997, **8**, pp. 825–829
[18] Carlson G., Lewis D., Mckinley K., *ET AL.*: 'Aerogel commercialization: technology, markets and costs', *J. Non-Cryst. Solids*, 1995, **186**, pp. 372–379
[19] Prakash S.S., Brinker C.J., Hurd A.J., *ET AL.*: 'Erratum: silica aerogel films prepared at ambient pressure by using surface derivatization to induce reversible drying shrinkage', *Nature*, 1995, **375**, p. 431
[20] Kocon L., Despetis F., Phalippou J.: 'Ultralow density silica aerogels by alcohol supercritical drying', *J. Non-Cryst. Solids*, 1998, **225**, pp. 96–100
[21] Baumann T.F., Gash A.E., Chinn S.C., *ET AL.*: 'Synthesis of high-surface-area alumina aerogels without the use of alkoxide precursors', *Chem. Mater.*, 2005, **17**, pp. 395–401
[22] Wu L., Huang Y., Wang Z., *ET AL.*: 'Fabrication of hydrophobic alumina aerogel monoliths by surface modification and ambient pressure drying', *Appl. Surf. Sci.*, 2010, **256**, pp. 5973–5977
[23] Horiuchi T., Osaki T., Sugiyama T., *ET AL.*: 'Maintenance of large surface area of alumina heated at elevated temperatures above 1300°C by preparing silica containing pseudo-boehmite aerogel', *J. Non-Cryst. Solids*, 2001, **291**, pp. 187–198
[24] Wang W., Zhang Z., Zu G., *ET AL.*: 'Trimethylethoxysilane-modified super heat resistant alumina aerogels for high-temperature thermal insulation and adsorption applications', *RSC Adv.*, 2014, **4**, (97), pp. 54864–54871


© The Institution of Engineering and Technology 2018

doi: 10.1049/mnl.2018.5077